

Forecasting Spacecraft Telemetry Using Modified Physical Predictions

Ryan Mackey¹ and Igor Kulikov¹

¹*Reasoning, Modeling, and Simulation Group, Jet Propulsion Laboratory,
California Institute of Technology, Pasadena, CA 91109, USA*

ryan.m.mackey@jpl.nasa.gov

kulikov@jpl.nasa.gov

ABSTRACT

Among systems that provide sensor data of their performance, one approach to prognostic estimation is *forecasting*, i.e. prediction of measurable parameters and comparison of predicted values against established operational limits. Forecasting can be attempted statistically, or can be based on rigorous physical simulation. However, combining these approaches is difficult where system mode behavior or timing of system activities is uncertain, limiting the accuracy or applicability of a forecast.

In this paper we describe a method to modify simulation outputs to better match current telemetry. We begin with a familiar autoregressive approach to model residuals between predicted spacecraft performance, provided by physics-based modeling tools, and up-to-date spacecraft telemetry. This result is then improved by transforming the simulation result to better fit recent data, and the transformation is applied to generate more accurate future predictions. The method is suitable for real-time signal prediction. We will motivate this approach and characterize its performance using example telemetry from the NASA Mars Exploration Rover spacecraft.*

1. INTRODUCTION

While spacecraft cannot be maintained in the classical sense, prognostics can be relevant to spacecraft operations, either to support activity planning or to detect and prevent operational trends that would lead to spacecraft safing. At present, trend analysis is usually

performed by hand, relying upon sophisticated physics simulation (Kordon and Wood, 2002).

Hand-driven analysis remains dependent on spacecraft telemetry, as do the simulations themselves. The spacecraft and its environment are difficult to simulate and may change dramatically in a short period of time. This is particularly true of spacecraft in complex environments such as landers or rovers. In addition, the physics models of the spacecraft response are often extremely complex and dependent upon dozens or hundreds of parameters, which precludes using them in a reactive manner. As a result, the simulations cannot be quickly adjusted if there is a sudden change in environment, a decision to reschedule or delay spacecraft activities, or an unexpected change in spacecraft state. Typically the simulation outputs, referred to as “predicts,” are updated only on a regular basis, at intervals of one to several days depending on the mission.

Simple statistical methods of trending such as autoregressive (AR) methods can react immediately to sensor updates or changes to planned behavior. AR-based approaches are often tried but may prove insufficient given the extreme complexity of spacecraft behavior, and may suffer from false alarms. The ideal balance from an operational perspective is a mixture of techniques that leverages deep physical understanding of spacecraft behavior, yet remains flexible and tailorable to fit sensor updates as they arrive. In this paper we describe one such approach, designed to modify the “predicts” in response to new data.

1.1 Prognostic Forecast Example: Mars Rover

A useful illustration is the thermal behavior of the Mars Exploration Rover (MER). Electronic components of the MER heat up when switched on and cool at their own individual rate when quiescent. Depending on

* This is an open-access article distributed under the terms of the Creative Commons Attribution 3.0 United States License, which permits unrestricted use, distribution, and reproduction in any medium, provided the original author and source are credited.

rover orientation, these components may be shaded, exposed to Martian wind, or loaded with additional solar radiation reflected from the ground or another part of the vehicle. Temperatures tend to follow a “daily” cycle that depends on the Martian season, latitude, and angle of terrain. In other words, the thermal state of electrical components is complex, and also highly dependent on the duration and timing of their operation.

Accurate signal prediction is particularly important for spacecraft prognostics for two reasons. First, where round-trip light time creates a significant delay in communication and control, operators can be warned of predicted violations of flight rules, which will lead to failures to execute commands and potentially strand the spacecraft in an undesirable state. One example is forecast of spacecraft component temperatures – if the components exceed preset temperature limits, a fault protection response will be triggered, rendering their function unavailable. Second, wear and component lifetime is dependent on operating conditions which cannot always be sensed with adequate fidelity. Signal forecasting, particularly in combination with physics-based models, can be used to provide much better estimates of the operating environment and support remaining life estimates. In addition to these functions, the signal forecasting approach presented here can be used to refine predictions of sequence execution and spacecraft state, relevant to activity planning and investigations of in-flight anomalies.

In our previous investigations, we demonstrated that forecasting MER thermal telemetry using time series analysis is possible but of limited potential accuracy (Mackey, James, and Kulikov, 2008). There are two main reasons for this: first, time series of telemetry data are not stationary; and second, there are spikes in temperature telemetry data caused by switching of component power. The occurrence of these spikes cannot be accurately predicted from telemetry data alone. These difficulties preclude a purely statistical forecast more than two steps ahead, or roughly ten minutes at best.

Fortunately, there is a sophisticated model available to predict power and thermal behavior of the MER. This model is used for activity planning but is problematic in mission analysis since the model data do not match the telemetry. These data are typically off both in time and absolute value, as shown in Figures 1 and 2, due to inevitable discrepancies between the model inputs and reality.

To illustrate and evaluate our hybrid approach, we will consider thermal telemetry data of Electronic Solid-State Power Amplifier (SSPA), Ultra High Frequency

(UHF) telecommunication components and of Rover Electronics Module (REM). We will contrast examples from two Solar days (Sols), numbers 13 and 434.

2. TECHNICAL DESCRIPTION

To begin, we assume that our data is composed of a background signal plus a superposed transient signal or series of signals. These transients correspond to planned activities, which may occur at a varying time, or may not occur at all.

A second important assumption is that it is the actual value, and not just the shape of the signal, that is important. This is intuitively obvious for temperature prediction, where exceeding a temperature limit could cause physical damage, and the spacecraft will automatically interrupt its operation to protect itself. This behavior is typical of numerous spacecraft subsystems, e.g. voltage and current limits, limits on orientation or motion of movable elements, etc.

Let us consider MER SSPA component temperature telemetry and the model data for Sol 13 (Figure 1). There are four separate SSPA activities, which are given by four spikes in the plot. To provide a telemetry forecast we have to take into account this specific SSPA activity. One possible way is to estimate the spikes and to include these activities in the physical model, as was done in this case. But there is a problem with this approach: We do not know when the modeled spikes will appear. Figure 1 clearly shows thermal and temporal differences between the actual telemetry (given by the blue dots) versus the model data (given by the red curve).

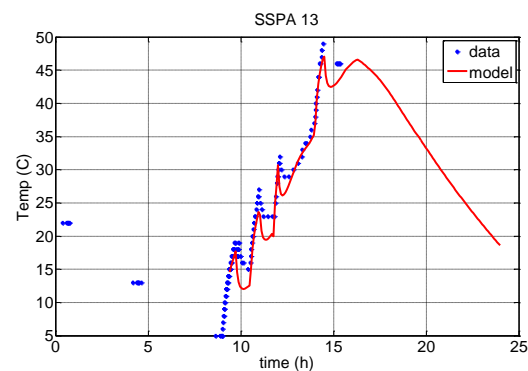


Figure 1: SSPA component temperature telemetry and model data for Sol 13

In addition to activity timing, differences are also caused by shifts in the background data, as shown in an

example of UHF temperature telemetry. MER UHF telemetry and the associated predict for Sol 434 are shown in Figure 2. The model data (given by the red curve) are shifted significantly with respect to the telemetry (the blue dots). Any prediction of maximum temperature or remaining operating margin based on this predict alone would be inaccurate as a result.

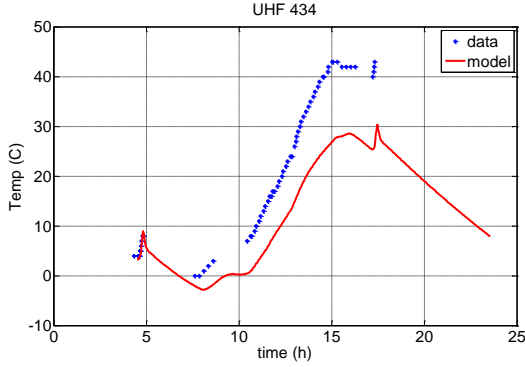


Figure 2: UHF component temperature telemetry and model data for Sol 434

As follows from Figures 1 and 2, the model data alone does not provide a particularly accurate forecast, especially where it is the value rather than the character of the signal that is important. In both of these examples, the model alone underpredicts the actual maximum temperatures experienced.

Nonetheless, the overall shape of the prediction is materially consistent with the actual telemetry. It should be possible to simply adjust the model data to get a better fit with actual telemetry. There is precedence for this approach, treating the problem as one of pattern recognition, allowing us to perform model modification as a transformation of 2D space (Duda and Hart, 1973). We can also look to modern approaches of image registration (Zitova and Flusser, 2003) for inspiration.

2.1 Transformation of model data

A model data curve is given by a function $y = y(t)$, where y is the temperature and t is the time. We will make a coordinate transformation as follows:

$$\begin{aligned} \bar{t}_i &= t_i + t_0 \\ \bar{y}_i &= b + ay_i \end{aligned} \quad (1)$$

We assume that the data are given as discrete set, a and b are simple coefficients, and t_0 is the time shift. Coefficients a , b and t_0 are found from a minimal

deviation of the model data from the telemetry. We will estimate a , b and t_0 in two steps.

First, given time t_0 , we compute the coefficients a and b from the system of equations below:

$$\begin{aligned} \bar{y}_1 &= b + ay_1 \\ \bar{y}_2 &= b + ay_2 \\ &\vdots \\ \bar{y}_N &= b + ay_N \end{aligned} \quad (2)$$

where \bar{y}_i and y_i ($i=1, \dots, N$) are telemetered values and the model data respectively. The solution of this system is given by:

$$[b \ a]^T = (A^T A)^{-1} (A^T \bar{Y}) \quad (3)$$

where $\bar{Y} = [\bar{y}_1, \dots, \bar{y}_N]^T$ is the array of telemetry, and the matrix A is constructed from the model data as follows:

$$A = \begin{bmatrix} 1 & y_1 \\ 1 & y_2 \\ \vdots & \vdots \\ 1 & y_N \end{bmatrix} \quad (4)$$

Solving equation (3) gives us the coefficients a and b that best modify the model curve. The accuracy of the model curve transformation to the telemetry can be measured by computing the average residual $\text{MEAN}(\bar{Y} - Y)$, and the standard deviation $\text{STD}(\bar{Y} - Y)$, where $Y = [y_1, \dots, y_N]^T$ is the array constructed with the model data, considering each element of the array as an independent measurement.

For the second step, we change the time shift t_0 , repeat the procedure to compute new values for a and b computation again and compute STD for time t_0 to see if the fit has improved. This search is motivated by the idea that mismatches between data and predictions will be primarily caused by a mismatch in timing of key events.

To find the best fit, we repeat the procedure several times. We assume that t_0 lies within an interval of K samples either shifted ahead or behind:

$$t_0 \in [-K\Delta t, -(K-1)\Delta t, \dots, (K-1)\Delta t, K\Delta t] \quad (5)$$

and compute $\text{MEAN}(\bar{Y} - Y)(k)$ and $\text{STD}(\bar{Y} - Y)(k)$ for times $t_0(k)$, ($k = -K, \dots, K$).

For our example, we will assume that activities, when they occur at all, happen within 15 samples of their expected time. Curves of MEAN and STD for SSPA Sol 13 for $K=15$ and $\Delta t = 0.01$ (hr) (or 0.6 (min)), are shown in Figure 3, below.

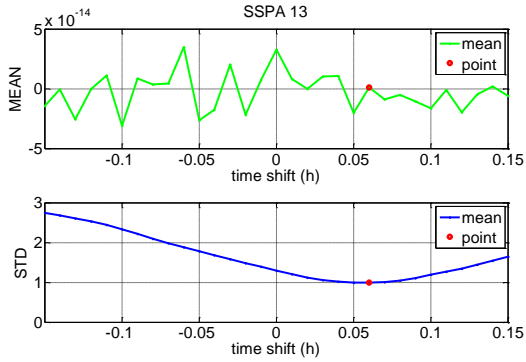


Figure 3: SSPA Sol 13 error MEAN and error STD as functions of time shift

The red dot in these plots corresponds to the k_0 - number of the best fit, defined as the shift that produces the smallest error STD (if there is more than one, the smallest shift should be chosen), as this represents the best match to signal behavior, and thus the most reliable prediction of future results. In the example above, this choice also minimizes error mean, but this will not necessarily be the case. A non-zero error mean at the chosen shift is acceptable if it is bounded, but a large error mean should be investigated further. This may indicate an insufficient sample window or structural differences between sensor data and the physics model.

For a given k_0 we estimate the time shift as $t_{shift} = k_0 * \Delta t$. After finding t_{shift} , we find the coefficients a and b which correspond to this time shift.

In this example, the best time shift is $t_{shift} = 0.06$ (hr) (Figure 3), the telemetry /model error mean is equal to zero, and error STD = 1. The coefficients a and b are found to be $a = 0.96$ and $b = 3.29$. Using these coefficients, the modified model data for SSPA Sol 13 is shown in Figure 4 (given by the black curve).

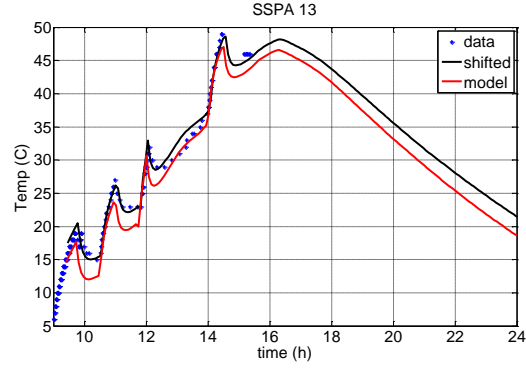


Figure 4: Telemetry (blue dots), model (solid red), and modified model (solid black) curves as functions of time

For a second example, we perform the same procedure for the UHF Sol 434 telemetry and model data. Curves of error MEAN and error STD for MER UHF Sol 434 are shown in Figure 5.

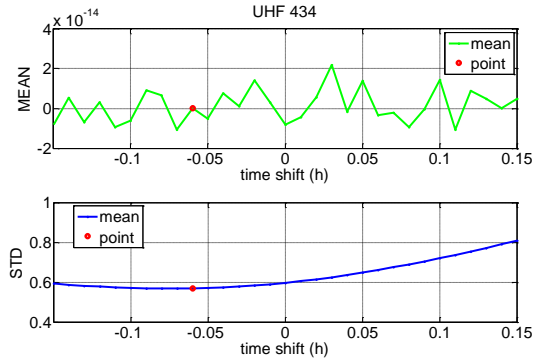


Figure 5: UHF Sol 434 error MEAN and error STD as functions of time shift

From Figure 5 it follows that minimal error STD corresponds to time shift of -0.07 hours. For this time shift, the mean of telemetry minus model data equals to zero, and the STD is equal to 0.55 degrees Celsius. The coefficients a and b are $a = 1.32$ and $b = 6.27$.

After applying this time shift and coefficient pair, we arrive at the modified model data curve shown in Figure 6. Telemetry and original data curves are shown in blue and red respectively. As before, this approach yields a dramatically improved prediction.

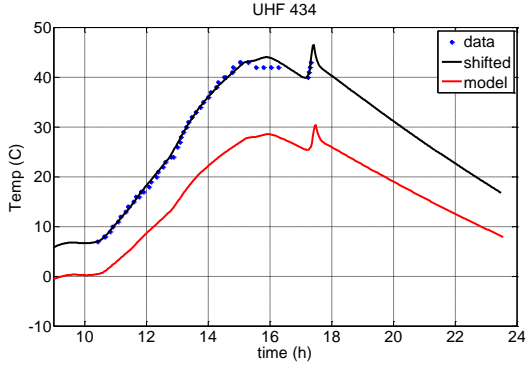


Figure 6: Telemetry (blue dots), model (solid red), and modified model (solid black) curves as functions of time

As these examples demonstrate, equation (3) provides satisfactory model data fitting for a variety of situations.

2.2 One step ahead forecast

The approach described above is not limited to *post facto* analysis, but can also be used for real-time prediction and monitoring. This approach also follows two steps.

To begin, we compute the telemetry-model data difference:

$$z_i = \bar{y}_i - y_i^{\text{model}} \quad (6)$$

where y_i^{model} are the modified model data described in Section 2.1. In Figures 4 and 6, these data are shown by the black curves.

Next, we treat the residual using AR(p) autoregressive estimation (Box et al., 1994; Brockwell and Davis 1996; Hamilton 1996). The parameters $\{w\}$ in this method are the weights in the equation given below:

$$z_i = w_1 z_{i-1} + \dots + w_p z_{i-p} \quad (7)$$

Once these weights are found, we apply them to the current set of telemetry data ($i=1, \dots, N_{\text{total}}$) to forecast the next expected value.

An example of this approach is shown in Figure 7, demonstrating the result applied to the SSPA data of Sol 13. The blue curve is the true residual $z_i = \bar{y}_i - y_i^{\text{model}}$, and the red curve is the forecasted residual, one sample ahead of its arrival.

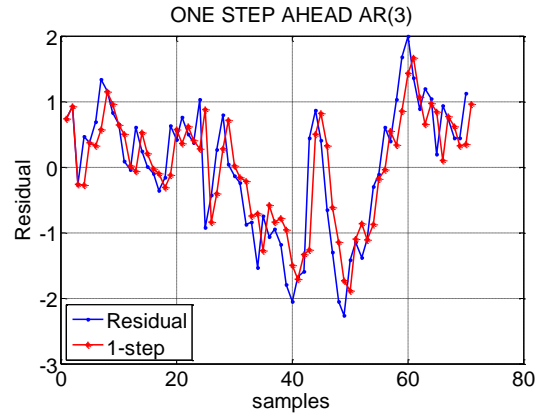


Figure 7: SSPA Sol 13 z data (red curve) and one step ahead forecast (red curve)

Similar results applied to the UHF data of Sol 434 are shown in Figure 8.

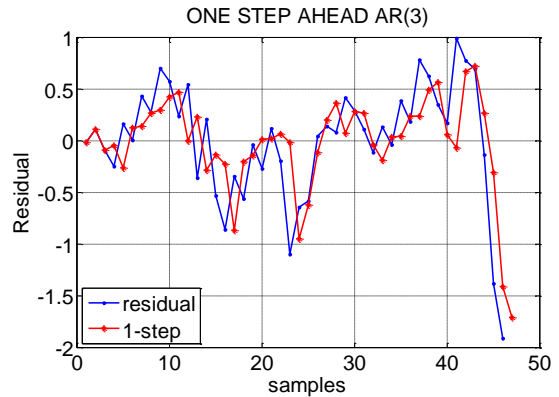


Figure 8: UHF Sol 434 z data (red curve) and one step ahead forecast (red curve)

After we have computed the forecast of the residual time series $\{z_i\}$, we can reconstruct the actual telemetry values $\{\bar{y}_i\}$ as $\hat{\bar{y}}_i = \hat{z}_i + y_i^{\text{model}}$, where $\hat{\bar{y}}_i$ is the telemetry forecast, \hat{z}_i is z_i -data forecast, y_i^{model} is the modified model data. In Figure 9 we present the final result for SSPA Sol 13.

The result for SSPA Sol 13 one step ahead forecast is the following: Forecast error MEAN is 0.01 (degrees Celsius) and STD is 0.56 (degrees Celsius).

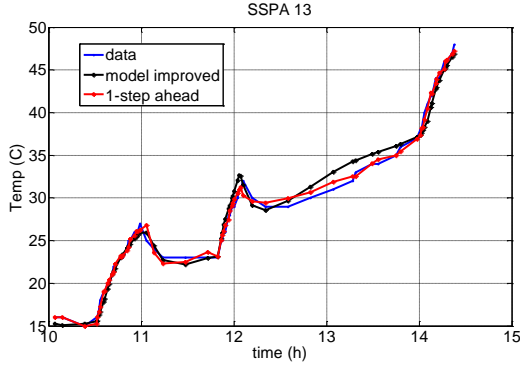


Figure 9: SSPA Sol 13 telemetry (blue curve), modified model data (the black curve), and one step ahead forecast (the red curve)

In Figure 10 we present the telemetry, the modified model and one step ahead forecast curves for the UHF temperature telemetry on Sol 434.

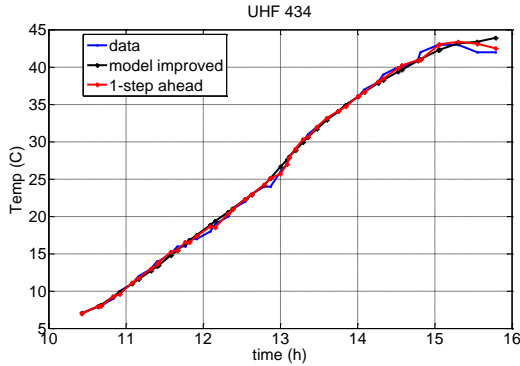


Figure 10: UHF Sol 434 telemetry (the blue curve) modified model data (the black curve) and one step ahead forecast (the red curve)

The result for UHF Sol 434 one step ahead forecast is the following: Forecast error MEAN is -0.01 (degrees Celsius) and STD is 0.41 (degrees Celsius).

The results presented above are similar to those taken on other systems. Tables 1 and 2 below summarize temperature forecast accuracy (still limited to only a single sample) for the SSPA, UHF, and REM components of MER.

Sol 13	
<i>REM</i> Temperature Forecast	
Error MEAN = 0.04 (C); STD = 0.44 (C)	
$t_{shift} = 0.28$ (hr); $a = 0.96$; $b = 3.23$	
<i>SSPA</i> Temperature Forecast	
Error MEAN=0.01 (C); STD =0.56 (C)	
$t_{shift} = 0.05$ (hr); $a=0.96$; $b=3.29$	
<i>UHF</i> Temperature Forecast	
Error MEAN =0.00 (C); STD=0.40 (C)	
$t_{shift} = 0.35$ (hr); $a=1.09$; $b=2.7$	

Table 1: One sample ahead forecast accuracy for Sol 13 MER data

Sol 434	
<i>REM</i> Temperature Forecast	
Error MEAN = -0.02 (C); STD=0.29 (C)	
$t_{shift} = 0.2$ (hr); $a = 1.16$; $b = 7.686$	
<i>SSPA</i> Temperature Forecast	
Error MEAN = 0.03 (C); STD = 0.43 (C)	
$t_{shift} = -0.05$ (hr); $a = 1.095$; $b = 7.844$	
<i>UHF</i> Temperature Forecast	
Error MEAN = -0.01 (C); STD = 0.41(C)	
$t_{shift} = -0.07$ (hr); $a = 1.32$; $b = 6.27$	

Table 2: One sample ahead forecast accuracy for Sol 434 MER data

As follows from the tables, the maximal MEAN does not exceed 0.04 (degrees Celsius) and the maximal STD of the forecast does not exceed 0.56 (degrees Celsius). This is for an admittedly short forecast time; however, it does include periods of complex operation and nonlinear signal behavior, and is vastly superior to the accuracy afforded by either physics modeling or statistical trending alone.

The forecasting method presented here can be extended using the AR(p) parameters, limited only by stability of the AR(p) filter. We will consider this more general case in the following section.

3. REAL-TIME FORECASTING

In the previous section, we investigated how to use the model data for the telemetry forecast improvement and found that we can avoid inaccuracies raised by partially unpredictable spacecraft activities by modifying the model data for the best fit to the telemetry. In this section we consider the problem of a real-time forecast. We assume that during the forecast, sensor data are measured on-board or telemetered to the ground and updated at a certain frequency. When we have obtained a number of data samples sufficient to fill an observation window (for our examples, we assume an initial window size of 25 samples), we can start to adjust the model curve and provide an updated forecast. This forecast procedure can be performed with the following steps:

- Step 1: Obtain N samples of the telemetry data
- Step 2: Adjust the model data as a best fit to the telemetry
- Step 3: Compute AR(p) coefficients and provide forecast
- Step 4: When the next telemetry data sample arrives, adjust the model data as the best fit to the new $N+1$ sample telemetry data set and provide forecast again

This process continues as long as desired. The sample window used to compute the forecast can be allowed to grow or can be fixed in size, gradually dropping old data, if needed for reasons of computational speed.

We will illustrate this process using the SSPA Sol 13 data, as it is the most challenging example considered here. We begin with the one step ahead telemetry forecast as described above. After collecting 25 samples of telemetry data, we begin adjusting the model data and compute the AR(3) parameters to begin our forecast. For this example, we will expand the window size every time new telemetry arrives. The results of the forecast are the following:

Model curve adjustment MEAN and STD of a and b coefficients, as the window grows in size to cover an entire Sol of operation, are shown in Figure 11. Over time, we find that both a and b fluctuate, but remain bounded, according to different “stretching” of the spacecraft activity timeline at different times of operation. Parameters a and b are also not independent, which is expected given their physical meaning. Statistics on these coefficients are as follows:

- a) MEAN (a) is 0.897 STD (a) is 0.021;
- b) MEAN (b) is 4.751 STD (b) is 0.395

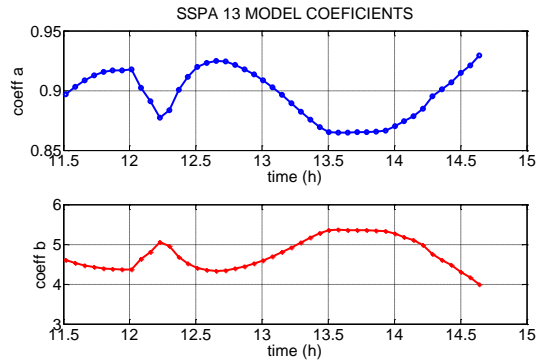


Figure 11: Change of the coefficients a and b over a full Sol of operation

As before, we also find the optimal time shift at each sample. The time shift MEAN is 0.06 (hr), STD of the time shift is 0.012 (hr).

The computed real-time one step ahead forecast, plotted against actual telemetry and the original model data for SSPA Sol 13 are shown in Figure 12. In this plot the telemetry data are shown by the blue curve, the forecast is the black curve and the original model data are the red curve. Forecast look ahead time is 0.07 (hr) or 4.3 (min). The first 25 points of telemetry data, required to start the forecast, are highlighted with magenta dots.

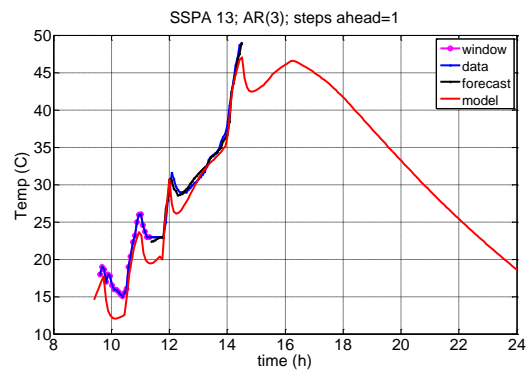


Figure 12: SSPA Sol 13 telemetry (blue curve) one-step ahead forecast (black curve) and model data (red curve)

For Figure 12, mean and standard deviation of the forecast data in comparison to telemetry are as follows: Forecast MEAN is 0.13 (degrees Celsius) and STD is 0.74 (degrees Celsius).

Finally, we present an example with our forecast extended to 13 minutes. This forecast is computed by extending the AR(3) prediction by three samples and reconstructing using the modified model data as before. The forecast of SSPA Sol 13 is shown in Figure 13; telemetry data are shown in blue, the forecast is shown in black, and the original model data are shown in red. As before, the first 25 points of telemetry data are required to start the forecast, as shown by the magenta dots.

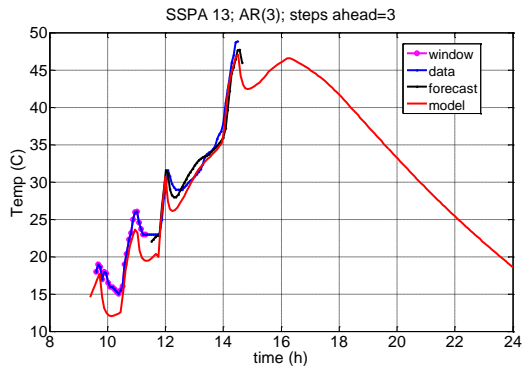


Figure 13: SSPA Sol 13 telemetry (blue curve) three steps ahead forecast (black curve) and model data (red curve)

Mean and standard deviation of the forecast data in comparison to telemetry are: Forecast MEAN is 0.27 (degrees Celsius) and STD is 1.3 (degrees Celsius). As follows from Figures 12 and 13, there remain no forecast errors related to electronic switching behavior. We have successfully removed these errors by including additional information about the SSPA and its planned behavior using the physical model predict.

3.1 Limitations of Technique

The approach presented here is extremely flexible and applicable to a wide variety of sensor data. However, like any attempt at curve-fitting, it can provide misleading or inaccurate results if pushed beyond prudent limits. A few guidelines for application of this method are as follows:

1. Time shift should be restricted to an interval no longer than the characteristic time of a single operation. Otherwise, the algorithm may attempt to fit one operation in a sequence to a different one entirely.
2. Wherever possible, confirm that modeled activities actually take place as planned. If the spacecraft activity deviates sufficiently from the original plan, any precomputed predict

may be worse than useless, and should not be used for prediction.

3. Test the AR(p) filter for stability, and limit the maximum look ahead accordingly. By adjusting the predict and reducing the magnitude of residuals, the forecast presented here is much less sensitive to error in the autoregressive parameters. However, even minimized, the autoregressive approach can yield unstable solutions if extended too far into the future.

4. CONCLUSION

In this research we present a method of telemetry forecast improvement using physical model predictions alongside of recent sensor data. This approach formalizes the concept of adjusting the model predict, both in absolute magnitude and timing of key features, to reduce the discrepancies between actual data and predicted data. These residuals are then treated statistically to produce an accurate forecast of future values. To evaluate this approach, we considered examples of thermal data from the Mars Exploration Rover mission, focusing on the temperature behavior of SSPA, UHF and REM components during two different cycles of operation.

As demonstrated above, we found that the standard deviation of the resultant forecast versus actual telemetry data does not exceed 1 degree Celsius – the limit of sensor resolution -- for up to three steps ahead (12.8 min in advance) for SSPA Sol 13 using this method.

While this style of forecast differs from that found in prognostic-driven maintenance, it is still of considerable value to spacecraft operations. A forecasted warning of only a few minutes, if available on board, could practically eliminate spacecraft safing events brought on by spacecraft activity and underestimated performance margin. This predictive ability also provides spacecraft operators with advance warning of problems and a rapid quantification of anomaly severity.

This approach could potentially be adapted to treat less dynamic prognostic data, for example the expected versus estimated lifetime performance curve of a component experiencing wear. The underlying assumptions allow for virtually any kind of physical model or sensed quantity. At present, our approach has only been tested upon examples of directly sensed physical quantities, but has been found to perform well on a variety of difficult signals.

ACKNOWLEDGMENT

This research was conducted at the Jet Propulsion Laboratory, California Institute of Technology, under a contract with the National Aeronautics and Space Administration. Government support for this effort is gratefully acknowledged.

REFERENCES

- G. E. P. Box, G. M. Jenkins, G. C. Reinsel (1994). *Time Series Analysis: Forecasting and Control*. Prentice-Hall, Inc.
- P. J. Brockwell, R. A. Davis (1996). *Introduction to Time Series and Forecasting*, Springer.
- R. O. Duda and P. E. Hart (1973). *Pattern Classification and Scene Analysis*, John Willey & Sons.
- J. D. Hamilton (1994). *Time Series Analysis*, Princeton University Press.
- M. Kordon and E. G. Wood (2002). Multi-mission Space Vehicle Subsystem Analysis Tools, in *Proceedings of the IEEE Aerospace Conference*, Big Sky, MO.
- R. Mackey, M. James, and I. Kulikov (2009). Prognostic Reasoning with Missing and Uncertain Data for Spacecraft Systems, in *Proceedings of the 2008 PHM Conference*, Denver, CO.
- R. Mackey and I. Kulikov (2009). Template Matching Approach to Signal Prediction, *NASA Tech Briefs*, in press.
- Barbara Zitova and Jan Flusser (2003). Image Registration Methods: A Survey, *Image and Vision Computing*, Elsevier, vol. 21, no. 11, pp. 977-1000.